Available online at www.sciencedirect.com

ScienceDirect

Neuromuscular Disorders 25 (2015) 835–842

www.elsevier.com/locate/nmd

Novel mutations in *DNAJB6* gene cause a very severe early-onset limb-girdle muscular dystrophy 1D disease

Johanna Palmio [a,*], Per Harald Jonson [b], Anni Evilä [b], Mari Auranen [c], Volker Straub [d], Kate Bushby [d], Anna Sarkozy [d], Sari Kiuru-Enari [c], Satu Sandell [a,e], Helena Pihko [f], Peter Hackman [b], Bjarne Udd [a,b,g]

[a] *Department of Neurology, Neuromuscular Research Center, University of Tampere and Tampere University Hospital, Tampere, FIN-33014, Finland*
[b] *Folkhälsan Institute of Genetics and the Department of Medical Genetics, Haartman Institute, University of Helsinki, Helsinki, Finland*
[c] *Department of Neurology, Unit for Neuromuscular Diseases, Helsinki University Central Hospital, Helsinki, Finland*
[d] *The John Walton Muscular Dystrophy Research Centre, Institute of Genetic Medicine, Newcastle University, Newcastle upon Tyne, UK*
[e] *Department of Neurology, Seinäjoki Central Hospital, Seinäjoki, Finland*
[f] *Deparment of Child Neurology, Helsinki University Central Hospital, Helsinki, Finland*
[g] *Department of Neurology, Vaasa Central Hospital, Vaasa, Finland*

Received 21 April 2015; received in revised form 17 July 2015; accepted 20 July 2015

Abstract

DNAJB6 is the causative gene for limb-girdle muscular dystrophy 1D (LGMD1D). Four different coding missense mutations, p.F89I, p.F93I, p.F93L, and p.P96R, have been reported in families from Europe, North America and Asia. The previously known mutations cause mainly adult-onset proximal muscle weakness with moderate progression and without respiratory involvement. A Finnish family and a British patient have been studied extensively due to a severe muscular dystrophy. The patients had childhood-onset LGMD, loss of ambulation in early adulthood and respiratory involvement; one patient died of respiratory failure aged 32. Two novel mutations, c.271T > A (p.F91I) and c.271T > C (p.F91L), in *DNAJB6* were identified by whole exome sequencing as a cause of this severe form of LGMD1D. The results were confirmed by Sanger sequencing. The anti-aggregation effect of the mutant DNAJB6 was investigated in a filter-trap based system using transient transfection of mammalian cell lines and polyQ-huntingtin as a model for an aggregation-prone protein. Both novel mutant proteins show a significant loss of ability to prevent aggregation.

Keywords: Limb-girdle muscular dystrophy; DNAJB6 gene; Childhood-onset

1. Introduction

Autosomal dominant limb-girdle muscular dystrophies (LGMD1) are a clinically and genetically heterogeneous group of progressive muscle diseases characterized by muscle weakness predominantly affecting the proximal limbs. Eight genetically distinct forms of LGMD1 are identified to date [1]. The severity of the different disorders vary and, except of LGMD1B, these dominant forms are usually considered to have a later onset and milder course of the disease than the recessive LGMD2 forms. Most of the reported LGMD1D patients remained ambulatory even in late adulthood.

LGMD1D showed linkage to 7q36 in several Finnish families [2,3], and later *DNAJB6* was identified as the causative gene for the disease [4,5]. DNAJB6 belongs to a class of co-chaperones characterized by a J-domain in the N-terminus [5]. All four reported disease-causing coding mutations, p.F89I, p.F93I, p.F93L, and p.P96R, are located in the G/F-rich linker domain of DNAJB6 [4–8]. The previously reported mutations usually cause adult-onset, slowly progressive proximal muscle weakness. However, occasional patients with earlier onset have been reported, although in these patients the further evolution was moderate with loss of ambulation only after age 50 and without respiratory failure [7,8]. LGMD1D muscle pathology is characterized by abnormal protein accumulations and autophagic rimmed vacuoles [5],

* Corresponding author. Department of Neurology, Neuromuscular Research Center, Tampere University Hospital and University of Tampere, FIN-33014 University of Tampere, Finland. Tel.: +358 3 3116111; fax: +358 3 35516164.
E-mail address: johanna.palmio@uta.fi (J. Palmio).

http://dx.doi.org/10.1016/j.nmd.2015.07.014
0960-8966/

and was reported to show a rather selective pattern of muscle involvement on muscle imaging [9].

A Finnish family and a British patient have been studied extensively in the past due to severely progressive childhood-onset muscle disease and respiratory failure. Two novel mutations in the same codon of *DNAJB6* gene were identified. Functional studies indicate they are associated with a more severe loss of anti-aggregation capacity.

2. Patients and methods

2.1. Patients

In Finnish family A with four affected members (Fig. 1), three siblings and their mother, the mother's parents were reported to be healthy. The mother had died at age 32 due to respiratory insufficiency. From the age of 14 years, she underwent repeated clinical examinations, muscle biopsy and electromyography (EMG). Her three daughters were first examined in their early teens (aged 12–15 years). Several muscular dystrophies as well as myofibrillar and rimmed vacuolar myopathies had been ruled out earlier with genetic testing. Spirometry tests were performed in all patients and echocardiography in the three siblings.

The British patient BII:1, is a 37-year-old female with negative family history. After years of progressive muscle weakness around age 15, she underwent extensive investigations including skin biopsy (with normal COLVI labeling) and genetic testing especially for rimmed vacuolar and myofibrillar myopathies with normal results. Spirometry tests were done at ages 21, 31 and 33 years.

The study was approved by the IRB of Tampere University Hospital. All participants provided appropriate consent.

2.2. Muscle pathology

Muscle biopsies were obtained after informed consent from three patients (AII:2, AIII:1, BII:1) and AIII:1 had a muscle biopsy twice. Histochemical analysis were performed on cryosections using standard methods with hematoxylin and eosin, modified Gomori trichrome, reduced nicotinamide

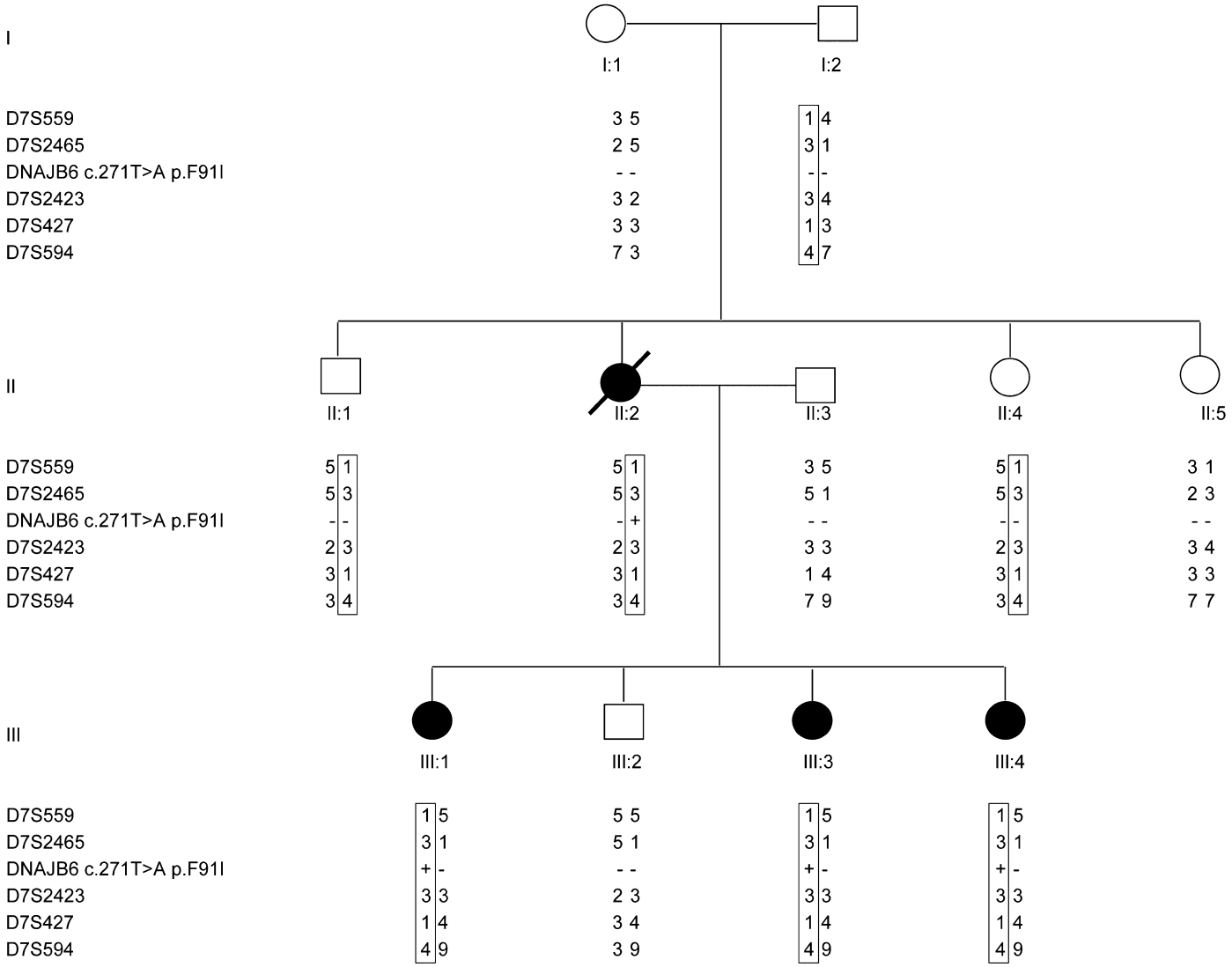

Fig. 1. Pedigree of the family A.

adenine dinucleotide-tetrazolium reductase (NADH-TR), and ATPase at pH 10.4, pH 4.6, and combined succinate dehydrogenase–cytochrome oxidase, (SDH–COX). For immunohistochemistry antibodies against the following proteins were applied: myosin fast, myosin slow, fetal and neonatal myosin heavy chains (clones NCL-MHCf, NCL-MHCs, NCL-MHCd and NCL-MHCn, Leica Biosystems, Newcastle, UK), MHC class I (M0736, Dako, Glostrup, Denmark), dystrophin (NCL-DYS2, Novocastra, UK), desmin (Biogenex, USA), myotilin (Novocastra, UK), and αB-crystallin (Novocastra, UK), DNAJB6 (Abnova, USA), LC3b (Cell Signaling technology, USA), p62 (Santa Cruz Biotechnology, USA). Ventana Benchmark automated immunostainer with DAB-detection was used for immunohistochemistry.

2.3. Genetic studies

Genomic DNA was extracted from blood by standard methods. Whole exome sequencing was performed on patients AIII:1 and AIII:3 at ATLAS Biolabs GmbH using SeqCap EZ Human Exome Library v2.0 (Roche NimbleGen) for DNA capture. The enriched DNA was sequenced with an Illumina HiSeq 2000 platform, 2x100bp. Reads were aligned to the human genome reference GRCh37/hg19 with Burrows–Wheeler Aligner and duplicate reads were removed with Picard [10,11]. The Genome Analysis Toolkit was used to realign the reads, recalibrate base quality scores and call variants [12]. Variants were annotated using wAnnovar and variants with frequency more than 1% in the 1000 Genomes or Exome Variant Server (ESP6500) databases were filtered out [13,14]. Variants present in both AIII:1 and AIII:3 were analyzed further.

Sanger sequencing was performed using DreamTaq™ DNA Polymerase (Thermo Scientific) according to standard protocol. Primers were designed using Primer3 software and PCR products were sequenced on an ABI3730xl DNA Analyzer (Applied Biosystems), using the Big-Dye Terminator v3.1 kit and analyzed with Sequencher 5.0 software (Gene Codes Corporation).

All family A members were genotyped for microsatellite markers D7S559, D7S2465, D7S2423, D7S427 and D7S594 spanning a region of 2.6 Mb around *DNAJB6*. Fluorescently labeled PCR products were analyzed using ABI3730xl DNA Analyzer and GeneMapper v4.0 software (Applied Biosystems). For patient BII:1 bidirectional sequencing analysis, using Mutation Surveyor software (v4.0.6), has been used to screen exons 2–10 of the DNAJB6 gene.

2.4. Plasmid constructs

The DNAJB6a, DNAJB6b, DNAJB6b p.F89I and DNAJB6b p.F93L and pEGFP/HD-120Q constructs have been described earlier [5,15]. The F91 mutations (c.271T > A, p.F91I and c.271T > C, p.F91L) were introduced to the pcDNA5/TO-DNAJB6b construct using site-directed mutagenesis. All constructs were verified by Sanger sequencing.

2.5. Functional studies

Filter-trap assays were performed essentially as described in reference 5. Briefly, T-REx 293 cells were co-transfected with pcDNA5/TO-DNAJB6 and pEGFP/HD-120Q constructs and induced after 4 h with 1 µg/ml tetracycline. Cells were harvested after 48 h and lysed in 750 µl FTA buffer (10 mM tris-HCl, pH 8.0, 150 mM NaCl, 50 mM dithiothreitol) containing 2% SDS and 1x Complete, triturated 5x through a 27G needle, sonicated at room temp for 1 min and heated to 98 °C. Sample for western blotting of soluble polyQ-HTT was taken and 100 µl of the lysate filtered with light suction through a 0.2 µm cellulose acetate membrane filter (Whatman GmbH). The filter was washed three times with 300 µl FTA buffer containing 0.1% SDS. The western blots and FTA membranes were stained using anti-V5 (Invitrogen) and anti-GFP (Santa Cruz) primary and Alexa Fluor-labeled (Invitrogen) secondary antibodies. The fluorescence was quantified using Odyssey software (LI-COR) and the aggregation score calculated from the levels of soluble and aggregated GFP-polyQ-HTT in induced and uninduced cells as: aggregation score = ($[\text{aggregated/soluble}]_{\text{induced}}/[\text{aggregated/soluble}]_{\text{uninduced}}$). Statistical significance was calculated as a two-tailed test using the Mann–Whitney U-Test Calculator in Excel. The *P*-values were not corrected for multiple testing.

3. Results

Clinical details and muscle investigations of the patients are presented in Table 1, and muscle strength evaluation (the Medical Research Council Scale, MRC) with muscle MRI findings in three siblings of Family A are shown in Table 2.

3.1. Family A

The age of onset of marked proximal muscle weakness was 10 to 12 years in most patients, although, three of them reported difficulties in running in early school ages. The disease progressed fast in the mother and she became wheelchair bound at age 27. She was unable to lift her arms, lumbar lordosis was marked and she had nasal voice but no dysphagia. She had severe restriction in the last spirometry and she died of respiratory failure at age 32 after having declined ventilatory support. The second eldest daughter (AIII:3) was the most severely affected; she had toe walking and ankle contractures already at age 6. Contractures were not observed in the others. The three siblings had all marked proximal lower limb weakness, which progressed to proximal upper limbs and to some extent also to distal lower limb muscles causing walking difficulties in early adulthood. CK levels were normal or slightly elevated. EMG was myopathic in all patients studied. Bone density test and cardiac evaluations showed normal results (at ages 20–24 years). All siblings had also dyspnea and showed mild to moderate restriction in spirometry (Table 1).

3.2. Patient BII:1

She had never been good in physical exercise and was unable to climb ropes or ride a bike. She underwent Achilles tendon release surgery due to ankle contractures and had a muscle

Table 1
Clinical data of the patients.

Feature	AII:2	AIII:1	AIII:3	AIII:4	BII:1
Age/sex	32*/F	24/F	21/F	20/F	37/F
Age of onset	10	13	6	<10	12
First symptoms	Running difficulties	Difficulties climbing stairs	Toe walking, ankle contracture	Running difficulties, climbing stairs	Toe walking, ankle contracture
Muscle weakness	Nasal voice, lumbar lordosis, prox UL, LL WCB (aged 27)	Neck flex, prox UL, LL Mild elbow flex/ext	Nasal voice, neck flex, prox UL, LL, elbow flex/ext Mild distal UL, LL	Neck flex, prox LL Mild prox UL, elbow flex/ext	Prox and distal LL > UL, neck, WCB (aged 28); Mild: facial, weak voice, pharyngeal weakness
CK levels	N-2 x UNL	1.5–2 x UNL	N	N	N
EMG	Myopathic (proximally)	Myopathic	Myopathic	Myopathic	NA
Muscle histology	Excess of fat, granular degeneration, vacuoles	Fibrosis, atrophy, necrosis, excess of fat, RV, myofibrillar aggregations	ND	ND	Fibrosis, atrophy, necrosis, excess of fat, RV, myofibrillar aggregations
Spirometry	FVC 1.42 (34%) FEV1 1.40 (33%)	FVC 2.63 (68%) FEV1 2.52 (74%)	FVC 2.47 (60%) FEV1 2.24 (61%)	FVC 2.79 (66%) FEV1 2.79 (73%)	Age 33: FVC 1.90 (47%) FEV1 1.73 (49%)

* Age at death.
F, female; UL, upper limbs; LL, lower limbs; WCB, wheelchair bound; CK, creatine kinase; UNL, upper normal limit; N, normal; EMG, electromyogram; NA, not available; RV, rimmed vacuoles; ND, not done; FVC, forced vital capacity; FEV1, forced expiratory volume in 1 second.

biopsy at the age of 12. Around age 15, she started to experience difficulties climbing stairs or getting up from the floor. She also reported distal weakness in her upper limbs. The proximal weakness increased over the years and she became fully wheelchair dependent at age 28. Minor contractures of neck, finger flexion and ankles were observed, as well as, spinal rigidity. Prominent distal wasting of upper and lower limbs was present. She had weak voice and dysphagia since age 20 but no cardiac involvement to date. CK was normal. Severe osteoporosis was diagnosed at age 32 after a fracture of right femur. FVC decreased constantly; at age 21: 2.71 liters (71%), at age 31: 2.21 liters (56%), and at age 33: 1.90 liters (47%).

Table 2
Muscle strength and imaging findings in three siblings of Family A.

Muscle strength according to MRC		III:1	III:3	III:4
Neck	Flexion	3	3 +	3 +
	Extension	5	5	5
Arm	Abduction	3 +	3	4
Elbow	Flexion	4	3 + /4−	4
	Extension	4 +	4−/3 +	4
Finger	Flexion	5	5−/4 +	5−
	Extension	5−	4/5−	5−
Hip	Flexion	3	3−	3 +
	Abduction	4	3	4 +
	Adduction	3 +	3−	4
Knee	Flexion	3 + /4−	4−	4−
	Extension	5−	4	5−
Ankle	Dorsiflex	5	4 + /4−	5−
	Plantarflex	5−	4 +	5
Degenerative changes on muscle MRI		Age 23, severe: Glut, Hamstrings, Gmed, Glat, S, D, Subscapularis	Age 17, severe: Glut, Hamstrings, Glat, S; moderate: Vastus muscles	Age 16, moderate: Glut, Hamstrings, Subscapularis

MRC, the Medical Research Council Scale; Glut, gluteus muscles; Gmed, gastrocnemius medialis; Glat, gastrocnemius lateralis; S, soleus; D, deltoideus.

3.3. Muscle imaging

All three siblings were examined by muscle MRI of the pelvis and lower limbs, and in AIII:1 and AIII:4 also of the upper limbs. Muscle MRI findings varied in severity (Table 2, Fig. 2), although, all of them had clear fatty degenerative changes more pronounced in the posterior thigh muscles and calf muscles. The most affected muscles were gluteal muscles, adductor magnus, long head of biceps femoris and in the lower legs gastrocnemius medialis and lateralis and soleus muscles. Vastus lateralis muscles were mildly to moderately affected in all patients. Iliopsoas was moderately degenerated in one patient. In the upper limbs of AIII:1, deltoid and subscapularis muscles were involved, and subscapularis to a lesser degree in AIII:4.

3.4. Muscle pathology

All biopsies showed dystrophic changes, i.e. fiber atrophy, necrosis, excess of fat and fibrosis (Table 1). In addition, there was marked rimmed vacuolar pathology in all samples. Myofibrillar aggregations were observed in the second biopsy from patient AIII:1 and in occasional fibers in BII:1. Myofibrillar aggregates stained strongly for myotilin and αB-crystallin and to somewhat lesser extent for desmin and dystrophin (Fig. 3A,B). Rimmed vacuoles were reactive for p62 and LC3b.

3.5. Genetics

Variants present in both AIII:1 and AIII:3 were analyzed from the whole exome sequencing data. Both AIII:1 and AIII:3 had a heterozygous missense mutation c.271T > A (NM_005494) in *DNAJB6* changing phenylalanine to isoleucine (p.F91I) in the same G/F-rich region where other known *DNAJB6* mutations are located.

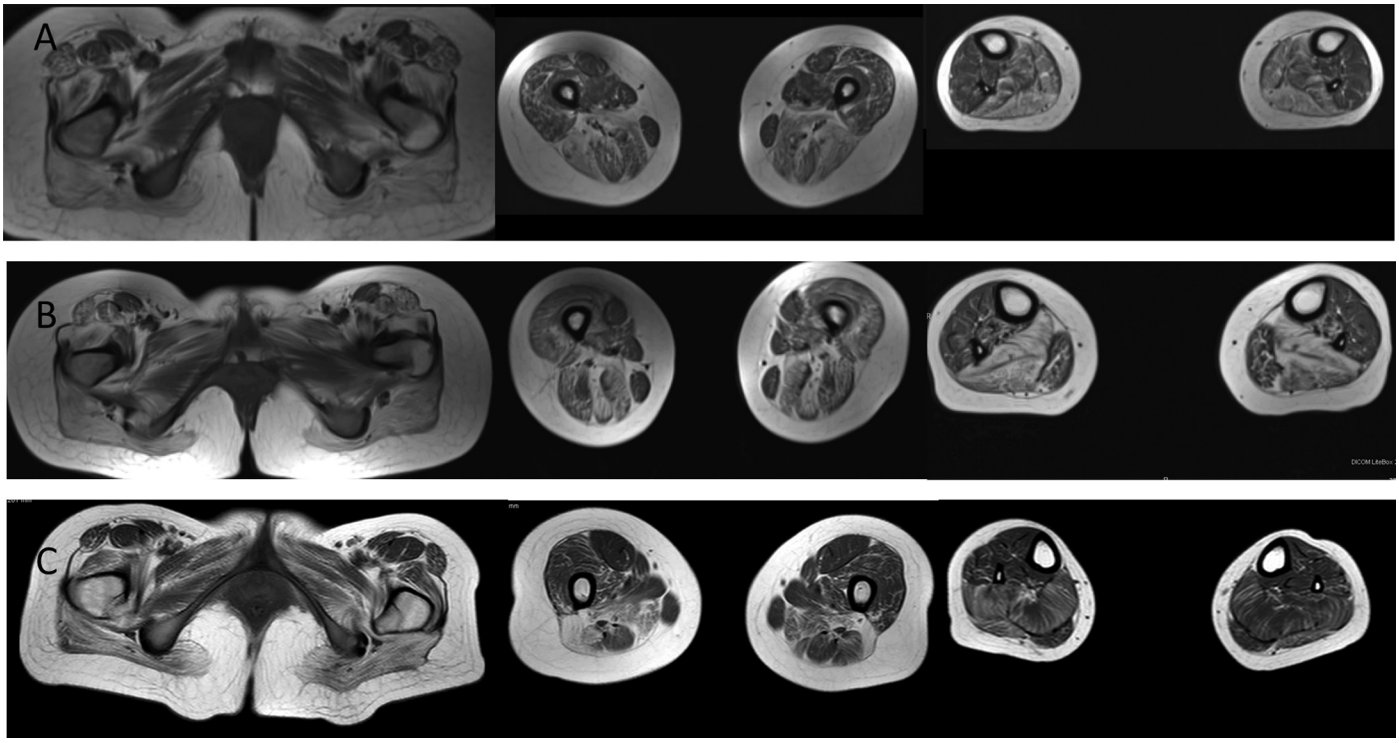

Fig. 2. Muscle MRI of the Finnish siblings. In all patients, severe fatty degenerative changes are seen in gluteal muscles, hamstrings (especially adductor magnus, semimembranosus and long head of biceps femoris), and calf muscles. Vasti muscles of the quadriceps are less severely affected, with sparing of rectus femoris, sartorius and gracilis. AIII:1 at age 23 (A), AIII:3 at age 17 (B): The patient has a more severe disease starting earlier than her siblings, and AIII:4 at age 16 (C).

All family A members were Sanger sequenced and genotyped. The *DNAJB6* mutation c.271T > A (p.F91I) segregated with the disease, being present in all affected members but not in any healthy ones, and it was found to be a de novo mutation in AII:2 based on haplotype segregation (Fig. 1).

DNA from BII:1 was analyzed by direct fluorescent sequencing for exons 2–10 of the *DNAJB6* gene. The patient was found to be heterozygous for the c.271T > C (p.Phe91Leu) variant in exon 5 of the *DNAJB6* gene.

3.6. Functional data

Both new mutations, p.F91I and p.F91L, show a significant reduction of the anti-aggregation function compared to the wild-type and p.F93L mutation (Fig. 4). The original p.F93L and p.F89I mutations are in this setup not significantly changed from wild-type b and wild-type a, respectively.

4. Discussion

The previously reported mutations in *DNAJB6* are known to cause adult-onset LGMD1D with mild to moderate progression and without respiratory muscle involvement [4–8]. The two novel mutations in *DNAJB6* reported here, however, cause severe childhood-onset disease with reduced walking, contractures and progressive respiratory insufficiency with a loss of ambulation in early adulthood.

Respiratory involvement has not been undoubtedly associated with the LGMD1D disease before. Only one patient, out of approximately 100, had dyspnea and sleep-associated breathing disorder with reduced FVC in mid-adulthood [7]. The two mutations in our patients caused marked respiratory problems already in early adulthood with important clinical relevance.

A pathognomonic pattern of muscle involvement on imaging has been reported in the patients with LGMD1D [9]. The first muscles involved in most patients have been soleus, adductor magnus, semimembranosus and biceps femoris followed by medial gastrocnemius, adductor longus and later vasti muscles of the quadriceps. Gluteal muscles were only mildly affected and later in the disease evolution. The same pattern could be identified in our patients in that marked soleus and hamstrings involvement was evident, although the early age of these changes and the more severe involvement of gluteal muscles, gastrocnemius lateralis and to a variable degree of vasti muscles of the quadriceps are new findings contributing to their earlier walking difficulties. In typical cases, gastrocnemius medialis has been involved earlier and lateralis later in the disease course [9]. The opposite was found in our patients whose gastrocnemius lateralis was more affected than medialis. The anterolateral compartment muscles in the lower legs were spared also in our patients. In the upper body, involvement of subscapularis seems to be quite a constant feature as it was observed in two of our patients and also earlier in LGMD1D patients [16]. Muscle pathology showed previously reported findings consisting of autophagic rimmed vacuolar degeneration and protein accumulations containing myotilin, desmin, αB-crystallin, and ectopic dystrophin, which overlap with myofibrillar myopathy. Muscle imaging findings and pathology in the patients in their teens were of the same severity as observed in

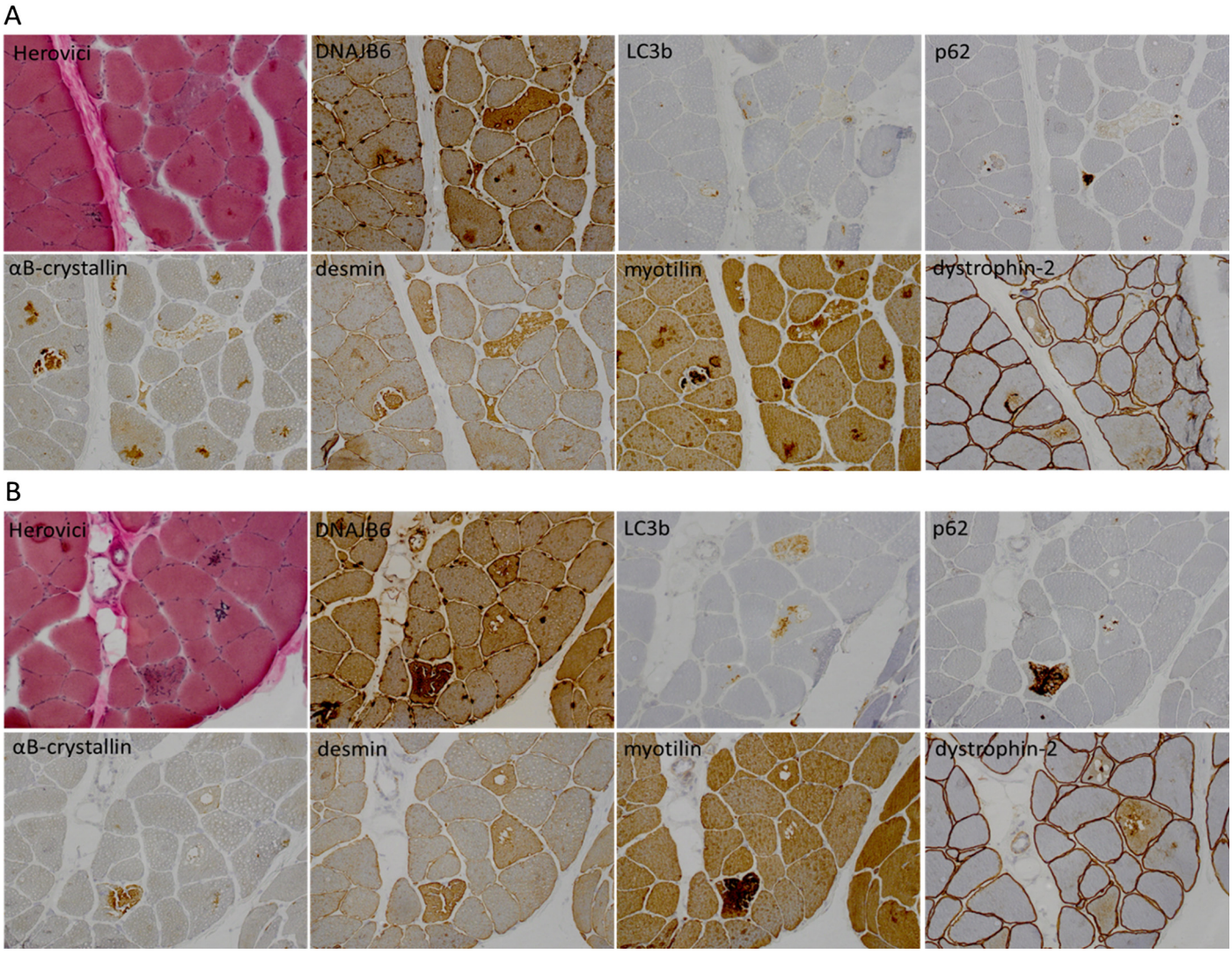

Fig. 3. Immunohistochemical stainings of tibialis anterior muscle of AIII:1. Figure 3A shows myofibrillar aggregates in several non-atrophic fibers that are reactive for DNAJB6. In these areas, there is a strong reactivity of αB-crystallin and myotilin with desmin and dystrophin-2 stainings showing less intensity. Figure 3B shows fibers with rimmed vacuolar pathology. Vacuolar fiber can show reactivity for myofibrillar proteins and in particular for autophagic degradation markers p62 and LC3b.

previously reported LGMD1D patients in their late adulthood emphasizing the difference in the phenotype severity.

DNAJB6 belongs to the evolutionarily conserved DNAJ/HSP40 family of proteins, which regulate molecular chaperone activity [17]. Mutations in *DNAJB6* have been shown to impair its ability to prevent aggregation of aggregation prone proteins [5]. Even if the detailed role of DNAJB6 in muscle is still largely unknown it has been shown to interact with components of the chaperone assisted selective autophagy (CASA) machinery and localize to the sarcomeric Z-disc. These interactions appeared unaltered by the previously reported mutations. We have earlier reported that the LGMD1D-mutations cause a reduction in DNAJB6's ability to prevent aggregation of polyQ-huntingtin [5]. The two new mutations cause a more severe loss of anti-aggregation function in transiently transfected cells compared to the originally reported p.F93L mutation, but less than the p.F89I mutation [5]. Our findings are compatible with the molecular mechanisms discussed earlier [5]. An understanding of the pathological changes in LGMD1D could yield therapeutic opportunities, such as silencing of the mutant allele or biochemically enhancing the anti-aggregation machinery.

5. Conclusions

The spectrum of clinical phenotypes is wider than previously reported and LGMD1D should definitely be included in the differential diagnosis of patients with childhood-onset progressive muscle weakness with or without respiratory symptoms and contractures.

Contributors

Study conception and design: Udd.

Execution and interpretation of the study: Palmio, Jonson, Evilä, Auranen, Straub, Bushby, Sarkozy, Kiuru-Enari, Sandell, Pihko, Hackman, Udd.

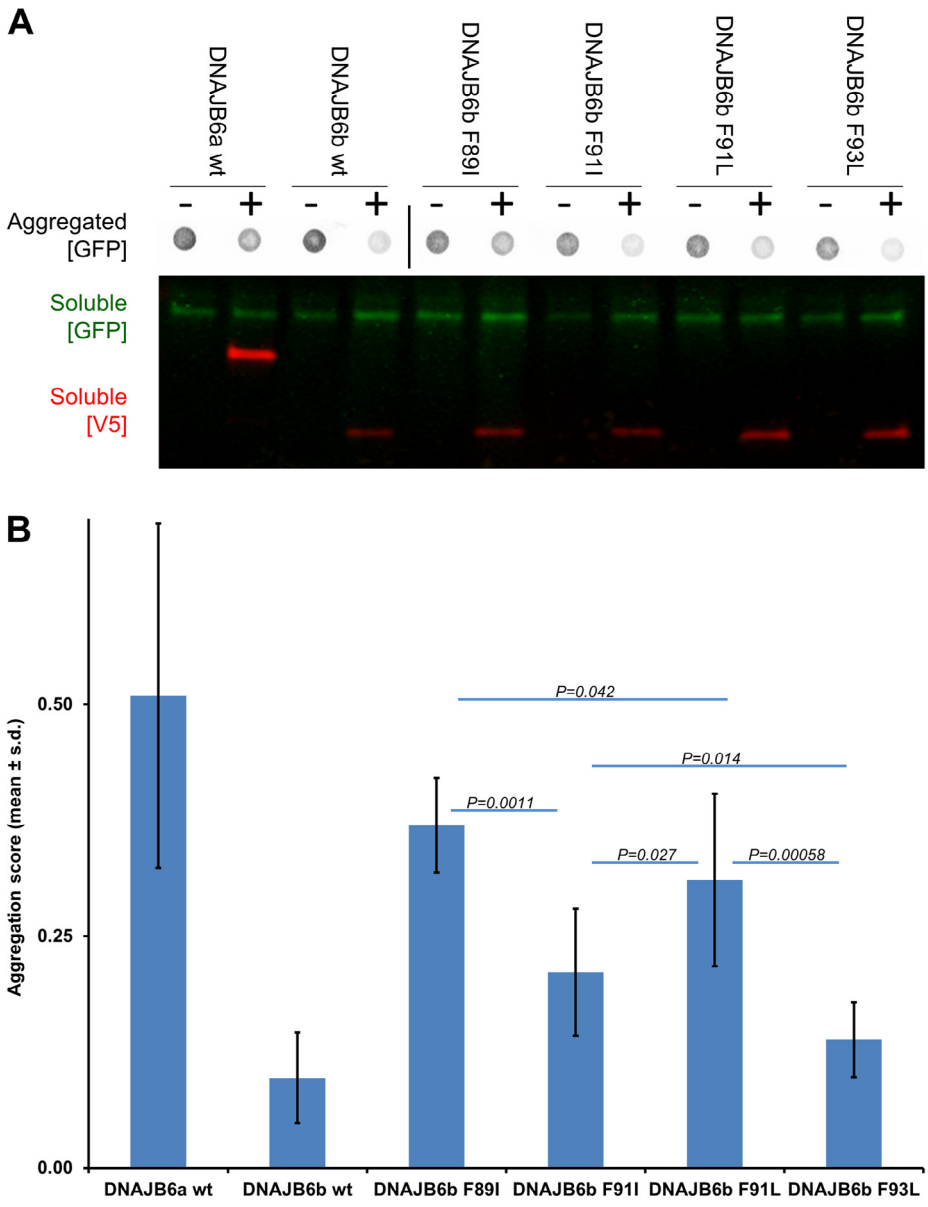

Fig. 4. Impaired anti-aggregation of mutant DNAJB6 proteins. A) GFP-tagged 120Q huntingtin was coexpressed with inducible V5-tagged DNAJB6 in induced (+) or uninduced (−) T-REx 293 cells. Soluble and aggregated polyQ-huntingtin was quantified by blotting of GFP and V5. In B), the aggregation score was calculated as the ratio of insoluble versus soluble polyQ-huntingtin in induced versus uninduced cells. The DNAJB6a and DNAJB6b wt constructs serve as negative and positive controls respectively. The new F91 mutations both show an increased loss compared to the original F93L, but less than the F89I mutant. The *P*-values are calculated by a two-sided Mann–Whitney U-test and n is 9 for each construct (three experiments in triplicate).

Funding

This work was supported by the Research Foundations of Vaasa Central Hospital (grant number 101016) and Tampere University Hospital (grant number 9R053) (BU).

Acknowledgements

We are grateful for the technical assistance of Helena Luque, Lydia Sagath, and Jaakko Sarparanta, Folkhälsan Institute of Genetics and the Department of Medical Genetics, Haartman Institute, University of Helsinki, Helsinki, Finland.

References

[1] Nigro V, Savarese M. Genetic basis of limb-girdle muscular dystrophies: the 2014 update. Acta Myol 2014;33:1–12.
[2] Sandell S, Huovinen S, Sarparanta J, et al. The enigma of 7q36 linked autosomal dominant limb girdle muscular dystrophy. J Neurol Neurosurg Psychiatry 2010;81:834–9.
[3] Hackman P, Sandell S, Sarparanta J, et al. Four new Finnish families with LGMD1D; refinement of the clinical phenotype and the linked 7q36 locus. Neuromuscul Disord 2011;21:338–44.
[4] Harms MB, Sommerville RB, Allred P, et al. Exome sequencing reveals DNAJB6 mutations in dominantly-inherited myopathy. Ann Neurol 2012;71:407–16.

[5] Sarparanta J, Jonson PH, Golzio C, et al. Mutations affecting the cytoplasmic functions of the co-chaperone DNAJB6 cause limb-girdle muscular dystrophy. Nat Genet 2012;44:450–5, S1-2.
[6] Sato T, Hayashi YK, Oya Y, et al. DNAJB6 myopathy in an Asian cohort and cytoplasmic/nuclear inclusions. Neuromuscul Disord 2013;23:269–76.
[7] Couthouis J, Raphael AR, Siskind C, et al. Exome sequencing identifies a DNAJB6 mutation in a family with dominantly-inherited limb-girdle muscular dystrophy. Neuromuscul Disord 2014;24:431–5.
[8] Suarez-Cedeno G, Winder T, Milone M. DNAJB6 myopathy: a vacuolar myopathy with childhood onset. Muscle Nerve 2014;49:607–10.
[9] Sandell SM, Mahjneh I, Palmio J, Tasca G, Ricci E, Udd BA. 'Pathognomonic' muscle imaging findings in DNAJB6 mutated LGMD1D. Eur J Neurol 2013;20:1553–9.
[10] Li H, Durbin R. Fast and accurate short read alignment with Burrows-Wheeler Transform. Bioinformatics 2009;25:1754–60.
[11] Broad Institute. http://broadinstitute.github.io/picard/>; 2015.
[12] McKenna A, Hanna M, Banks E, et al. The Genome Analysis Toolkit: a MapReduce framework for analyzing next-generation DNA sequencing data. Genome Res 2010;20:1297–303.
[13] Wang K, Li M, Hakonarson H. ANNOVAR: functional annotation of genetic variants from high-throughput sequencing data. Nucleic Acids Res 2010;38:e164.
[14] Chang X, Wang K. wANNOVAR: annotating genetic variants for personal genomes via the web. J Med Genet 2012;49:433–6.
[15] Hasholt L, Abell K, Nørremølle A, Nellemann C, Fenger K, Sørensen SA. Antisense downregulation of mutant huntingtin in a cell model. J Gene Med 2003;5:528–38.
[16] Tasca G, Monforte M, Iannaccone E, et al. Upper girdle imaging in facioscapulohumeral muscular dystrophy. PLoS ONE 2014;9:e100292.
[17] Ohtsuka K, Hata M. Mammalian HSP40/DNAJ homologs: cloning of novel cDNAs and a proposal for their classification and nomenclature. Cell Stress Chaperones 2000;5:98–112.